COPY

NASA
Contractor Report 185200

AVSCOM
Technical Memorandum 90-C-003

Computer Simulation of Gear Tooth Manufacturing Processes

AD-A227 148

Dimitri Mavriplis and Ronald L. Huston
University of Cincinnati
Cincinnati, Ohio

DTIC
ELECTE
OCT 0 5 1990
S B D

February 1990

Prepared for
Lewis Research Center
Under Grant NSG-3188

NASA
National Aeronautics and Space Administration

US ARMY
AVIATION
SYSTEMS COMMAND
AVIATION R&T ACTIVITY

DISTRIBUTION STATEMENT A
Approved for public release;
Distribution Unlimited

CONTENTS

	Page
ABSTRACT	1
1. INTRODUCTION	2
2. REVIEW OF SPUR AND BEVEL GEARS AND THEIR MANUFACTURE	3
2.1 External Spur Gears	3
2.2 Straight Bevel Gears	5
2.2.1 Milling	7
2.2.2 Hobbing	8
2.2.3 Shaping	9
3. DIFFERENTIAL GEOMETRY - ENVELOPES	10
3.1 Theoretical Considerations	10
3.2 Envelope of a One Parameter Family of Curves	12
3.3 Envelope of a Straight Sided Rack Cutter on the Gear Blank	14
4. ENVELOPE OF INVOLUTE PROFILE CUTTER	16
4.1 Introduction	16
4.2 Involute Analysis	17
4.3 Rolling Analysis	20
4.4 Envelope Analysis	22
4.5 Envelope of Involute	23
5. COMPUTER SIMULATION OF MANUFACTURING PROCESSES	28
5.1 Introduction	28
5.2 Gear and Straight Sided Rack	29
5.3 Involute Profile Cutter on a Wheel	35
5.4 Straight Bevel Gears	41
DISCUSSION	46
CONCLUSIONS	47
REFERENCES	48

ABSTRACT

This report discusses the use of computer graphics to simulate gear tooth manufacturing procedures. An analytical basis for the simulation is established for spur gears. The simulation itself, however, is developed not only for spur gears, but for straight bevel gears as well.

The applications of the developed procedure extend from the development of finite element models of heretofore intractable geometrical forms, to exploring the fabrication of nonstandard tooth forms.

Accession For
NTIS GRA&I ☑
DTIC TAB ☐
Unannounced ☐
Justification
By
Distribution/
Availability Codes
Dist | Avail and/or Special
A-1

INSPECTED 4

1. INTRODUCTION

This report discusses the geometry of gear tooth manufacturing procedures. It presents results of research supported by the National Aeronautics and Space Administration, Lewis Research Center under Grant NSF 3188 to the University of Cincinnati. It is based upon a portion of the first author's doctoral dissertation [1].

The gear tooth surface geometry is viewed as the envelope of a cutting tool as it sweeps through a gear blank. The analysis is based upon earlier research also supported by the Lewis Research Center and reported in [2,3].

Recently there have been dramatic advances in procedures for computer-aided design of mechanical systems. In particular, there have been significant advances in finite element methods and in associated computer graphic procedures. Indeed, in the past decade the finite element method and computer graphic analyses have become standard procedures in mechanical design.

For power transmission and gear design, however, the geometry has often precluded accurate applications of the finite element method. That is, the gear tooth profile is difficult to define -- especially for helical and bevel gears. The contact path of mating gears is even more difficult to obtain.

In this report we present a computer graphics technique for developing gear tooth geometry. It is based upon a geometric modeling of the gear fabrication procedure. That is, the gear tooth surface is viewed as the "envelope" of a gear

cutter passing through the gear blank. In the report we develop analytical procedures for determining the envelopes. These procedures in turn are used to validate computer graphic (numerical) methods for obtaining the envelopes.

The balance of the report is divided into five parts with the first part providing a brief review of spur and bevel gear generating processes. The next two parts discuss the envelopes of spur gear cutters. The subsequent part discusses a computer graphic technique for simulating the cutting process. The final part contains a brief discussion and concluding remarks.

2. REVIEW OF SPUR AND BEVEL GEARS AND THEIR MANUFACTURE

In the following paragraphs we review the nomenclature of spur and bevel gears. Their cutting and fabrication methods are also discussed.

2.1 External Spur Gears

The involute spur gear is the most predominant tooth profile used in power transmission devices. A spur gear and its rack are depicted in Figure 2.1.1.

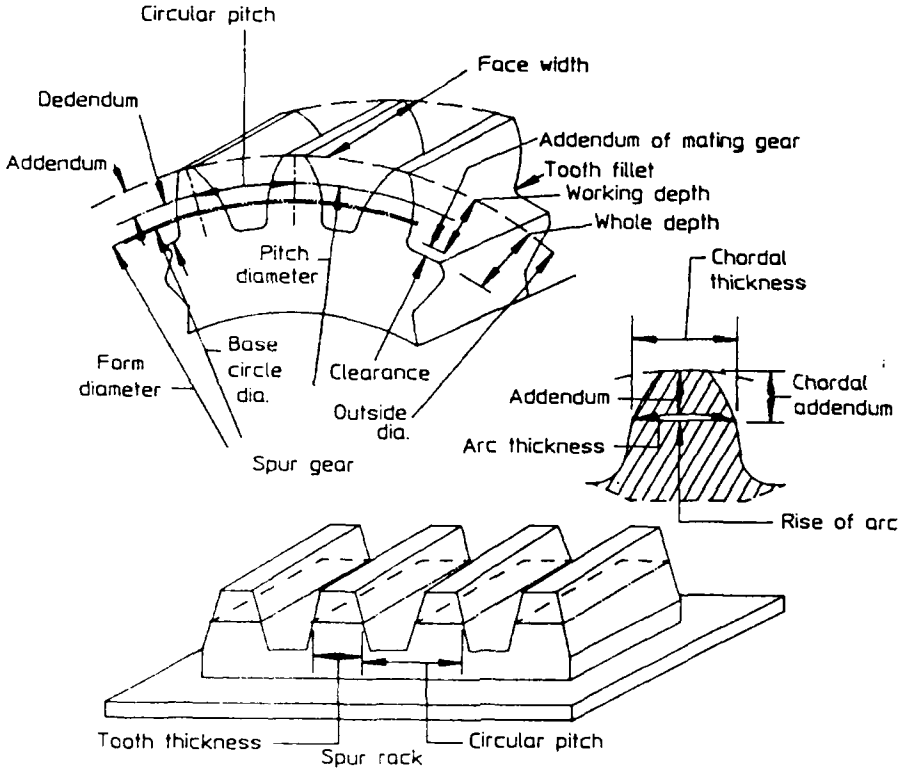

Figure 2.1.1 Spur Gear Nomenclature

The "involute" spur gear is so-named since the tooth profile has the shape of an involute curve. The cycloid is the only other curve affiliated with spur gear teeth. However, the cycloid tooth applications are limited to clocks and watches.

The involute profile has the advantage of easy manufacturability, and the kinematic feature that the velocity ratio of mating gears does not change as the center distance varies. Figure 2.2 depicts mating spur gears.

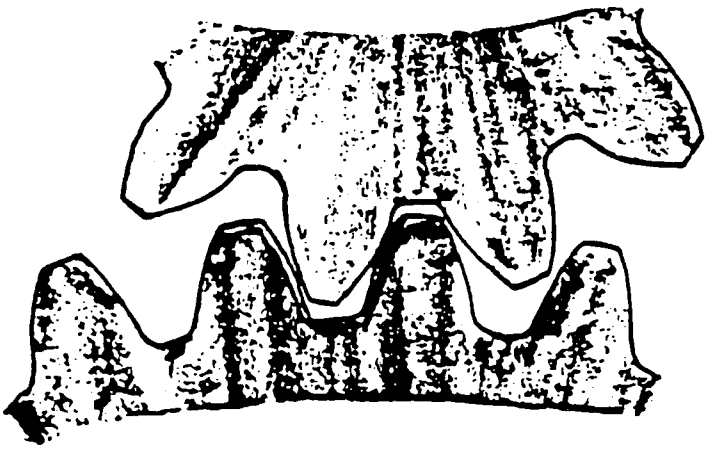

Figure 2.1.2 Mating Spur Gears

2.2 Straight Bevel Gears

Bevel gears are used in connecting shafts with intersecting axes. The pitch surface is conical. Rolling without slippage takes place between the pitch cones of the two mating bevel gears. The teeth are tapered in both thickness and height. The tooth profile in a section normal to the tooth, closely corresponds to that of a spur gear tooth with a pitch radius equal to the back cone distance, and a diametrical pitch equal to that of the bevel gear. Such a spur gear is called an "equivalent spur gear".

Bevel gear terminology and nomenclature are given in Figure 2.2.1.

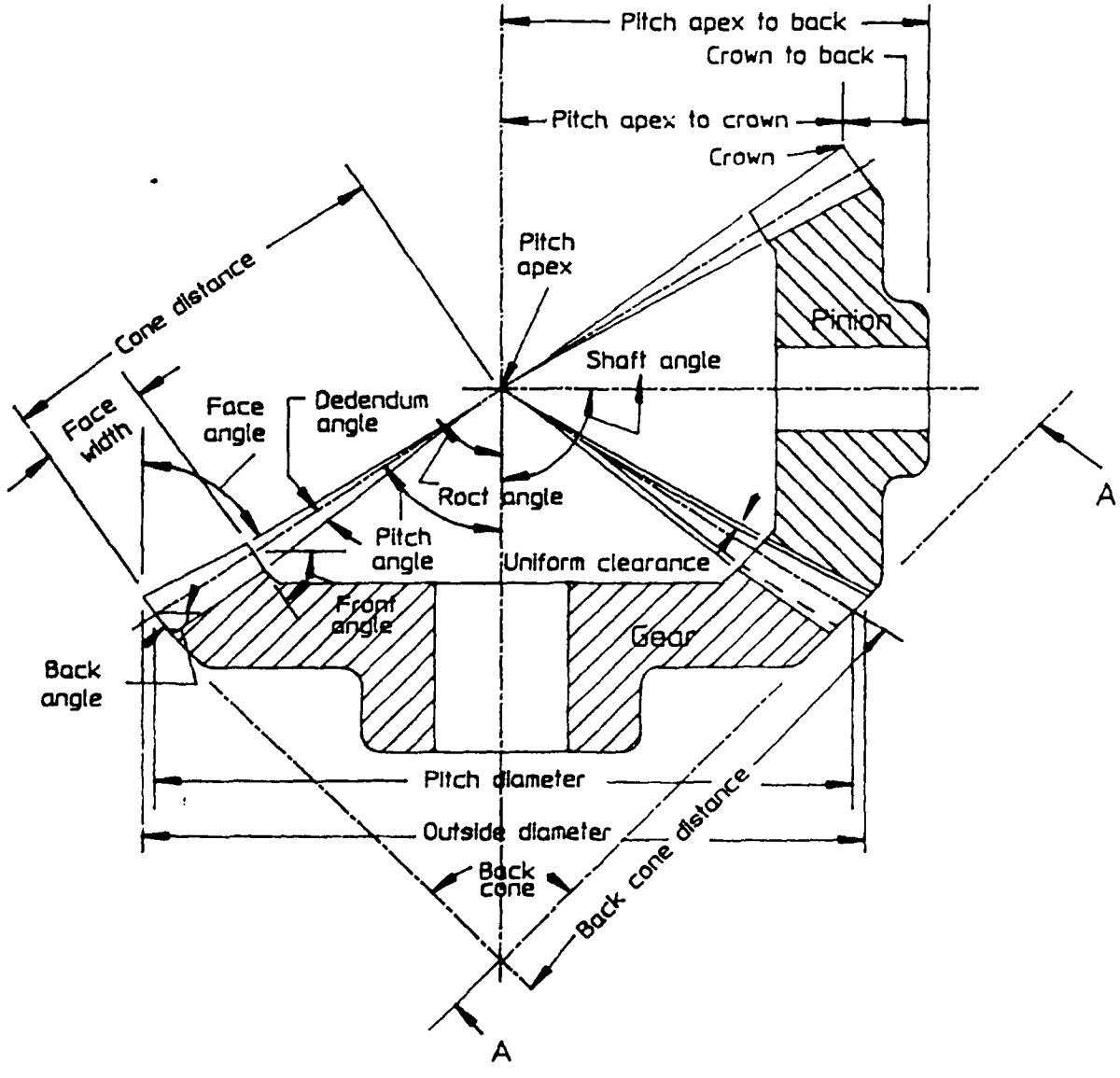

Figure 2.2.1 Bevel Gear Nomenclature

The equivalent spur gear nomenclature is presented in Figure 2.2.2.

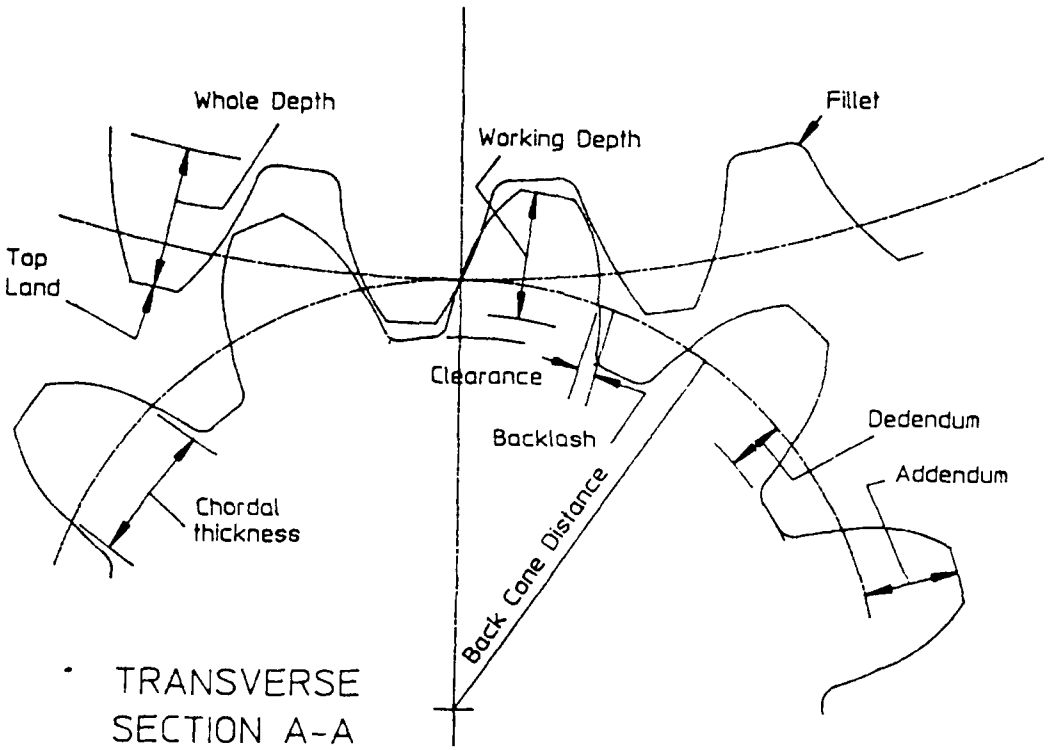

Figure 2.2.2 Equivalent Spur Gear Nomenclature

2.2.1 Milling

Gear milling produces spur gear teeth and straight bevel gear teeth using a form cutter. One tooth space is milled at a time. The gear blank is then indexed to the next cutting position. A disadvantage of this method is inaccurate tooth spacing.

Gear milling is a non-generating process.

Figures 2.2.1.1a and 2.2.1.1b show the milling cut of a spur and straight bevel gear tooth.

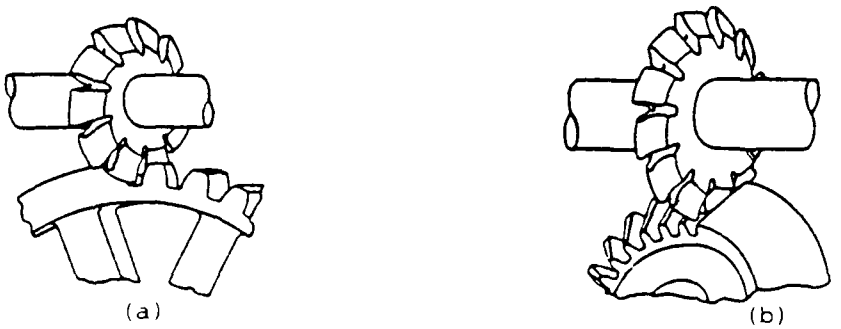

Figure 2.2.1.1 Milling of Spur and Straight Bevel Gear Teeth

2.2.2 Hobbing

Hobbing is a generating process of cutting spur gears. The gear teeth are gradually formed in a series of cuts. The generation of the gear tooth is a continuous indexing process in which both the cutter and the gear blank rotate in a constant ratio while the hob is fed into the gear blank. The most common shape of the hob has straight sides, thus producing involute spur gear teeth. Figures 2.2.2.1 depict the generation of a spur gear with a hob.

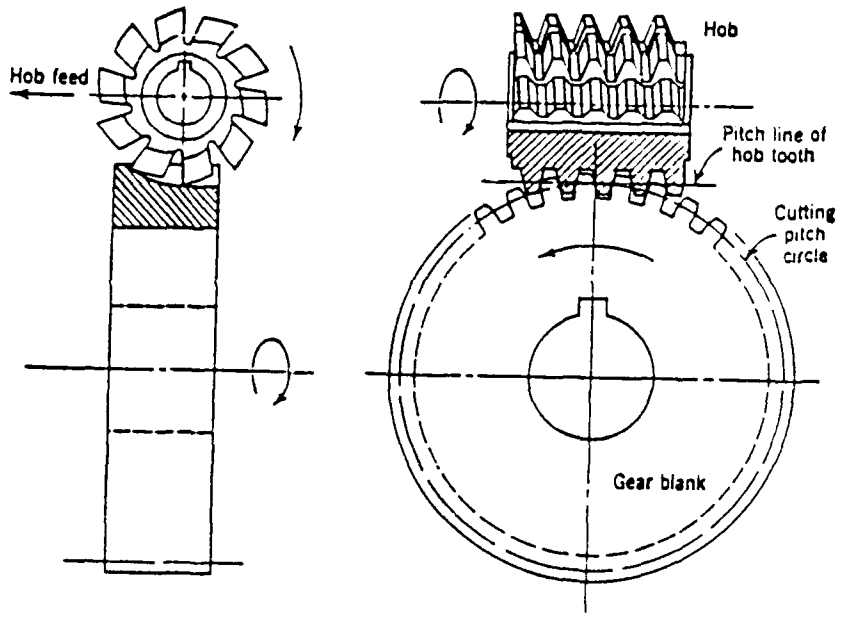

Figure 2.2.2.1 Spur Gear Hobbing

The constant indexing makes hobbing rapid and accurate. It is also economical since one hob will cut a number of teeth of a given pitch and pressure angle.

2.2.3 Shaping

Gear shaping is also a generating process. Here the cutter is a gear itself. It generates the proper tooth curve to mesh with itself. The cutter is rotated in a constant ratio with the gear blank. Using a reciprocating motion, material is then removed from the gear blank. A diagram depicting this process is shown in Figure 2.2.3.1, for spur gear teeth.

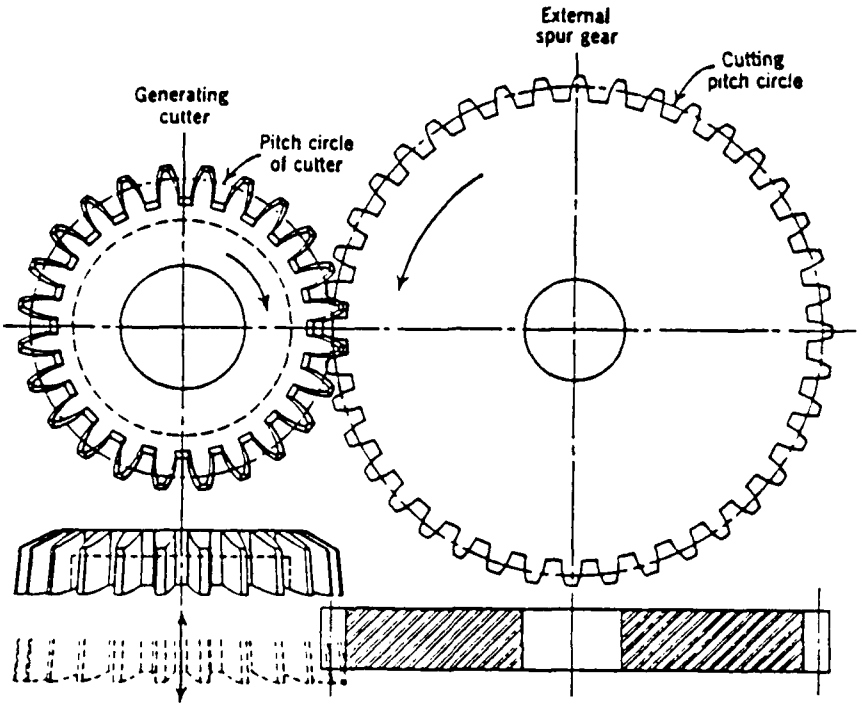

Figure 2.2.3.1 Shaping of Spur Gear

3. DIFFERENTIAL GEOMETRY - ENVELOPES

3.1 Theoretical Considerations

Consider a family of surfaces defined by the equation

$$f(x,y,z,t) = 0 \tag{3.1.1}$$

where t is the parameter. As t changes, a new surface member of the family is defined. Consider a typical surface, S, which intersects with a neighbor surface, S′, in a curve, C. If S and S′ correspond to the values t and t+Δt,

then the intersection C is described by the two equations

$$f(x,y,z,t) = 0 \quad \text{and} \quad f(x,y,z,t+\Delta t) = 0 \tag{3.1.2}$$

The surface

$$f(x,y,z,t+\Delta t) - f(x,y,z,t) = 0 \tag{3.1.3}$$

also passes through the curve C. Consequently, the curve C is described by the equations

$$f(x,y,z,t) = 0 \quad \text{and} \quad r(x,y,z,t) - f(x,t,z,t+\Delta t) = 0 \tag{3.1.4}$$

In the limit, as $\Delta t \to 0$ and S approaches S′, the curve C approaches a curve C′. C′ is defined by the equations:

$$f(x,y,z,t) = 0 \quad \text{and} \quad \frac{\partial[f(x,y,z,t)]}{\partial t} = 0 \tag{3.1.5}$$

As t varies, the curve C′ also varies, generating a surface called the envelope of the family [17]. The envelope is a surface tangent to each surface S of the family at all points of the curve C′ on S. The elimination of t, the parameter between f and $\frac{\partial f}{\partial t}$, produces an equation G(x,y,z) = 0, which precisely describes the envelope of the family.

As an example, consider the family of planes equidistant from a fixed point. It is readily seen that the envelope of this family is a spherical

surface with a radius equal to the distance of the plane from the fixed point. The family is a two-parameter family, since two angles are needed to determine the orientation of the plane relative to the point.

It is readily seen that deriving an equation that describes the envelope analytically is a complex process. In the following section, the development of an envelope for a one parameter family of curves is presented. Several examples are presented to demonstrate the use of this theory, the most advanced being the determination of the envelope of an involute profile cutter.

3.2 Envelope of a One Parameter Family of Curves

The best way to illustrate the application of the concepts presented in the previous section is to consider a simple case: a one parameter family of lines equidistant from a fixed point in a plane.

In Figure 3.2.1 a family of lines L, each a distance r from point O, are shown. The position of each line L can be defined by the single parameter ϕ.

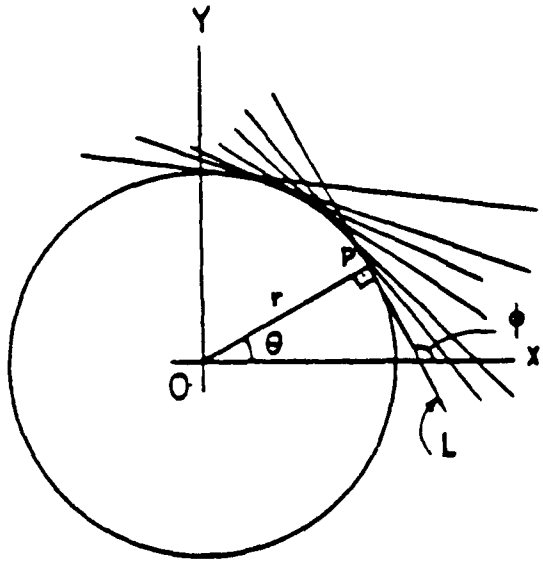

Figure 3.2.1 Family of lines equidistant from a point

The equation of L is a straight line

$$y - y_o = m\,(x - x_o) \tag{3.2.1}$$

where m is its slope and (x_o, y_o) are the coordinates of P, the point of intersection of L and its normal line through O. Since m is $\tan\phi$ and y is $r\sin\theta (= -r\cos\phi)$ and x_o is $r\cos\theta (= r\sin\phi)$, we can write 3.2.1 as

$$y + r\cos\theta = \tan\phi + (x - r\sin\phi) \tag{3.2.2}$$

or

$$y\cos\phi = x\sin\phi + r = 0 \tag{3.2.3}$$

This is the parametric representation of the family with ϕ as its parameter:

$$f(x, y, \phi) = 0 \tag{3.2.4}$$

Differentiating with respect to ϕ, we have:

$$\frac{\partial f}{\partial \phi} = -y\sin\phi + x\cos\phi = 0 \qquad (3.2.5)$$

Solving for x and y simultaneously in equations (3.2.3) and (3.2.5), we obtain the expressions

$$x = -r\sin\phi \qquad (3.2.6.a)$$

$$y = -r\cos\phi \qquad (3.2.6.b)$$

Substituting equations (3.2.6) into (3.2.3) and eliminating ϕ we have

$$y(-\frac{y}{r}) + x(-\frac{x}{r}) + r = 0 \qquad (3.2.7)$$

or

$$x^2 + y^2 = r^2 \qquad (3.2.7)$$

which is, as expected, the equation of a circle. This expression represents the equation of the envelope of the lines L.

3.3 Envelope of a Straight Sided Rack Cutter on the Gear Blank

S. Chang, R. L. Huston, and J. J. Coy [18] have developed an analytical expression for the involute tooth profile of a spur gear, generated by using a straight sided rack cutter as described in section 2.3.2. The results of this analysis are included in this section as an example of the theory discussed in

section 3.1. As an aid to visualizing this geometry, consider a perfectly plastic wheel rolling over a straight sided step. The impression of the step on the plastic wheel is the envelope of the family of line segments representing the side of the step. The only difference from the previous example is the fact that the wheel is rolling. Hence, it is advantageous to describe the geometry relative to a coordinate system fixed on the wheel (Figure 3.3.1).

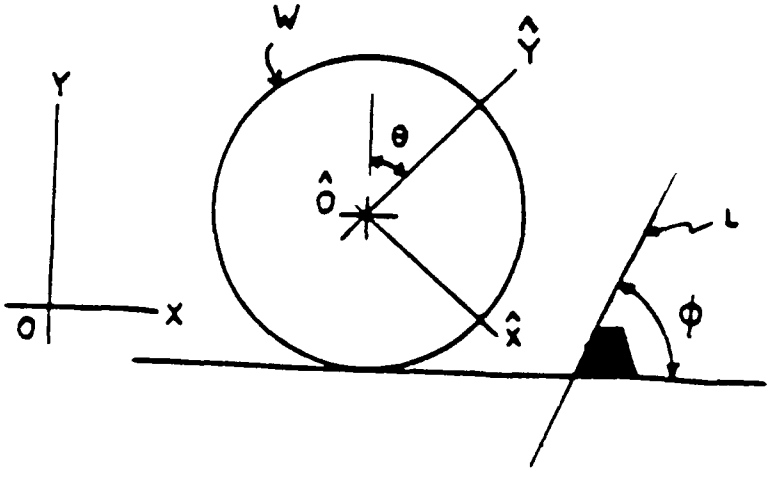

Figure 3.3.1 Wheel and step

The equations of the line and its derivative with respect to the parameter are found to be:

$$\hat{y}(\cos\theta - \tan\phi \sin\theta) - \hat{x}(\sin\theta + \tan\phi \cos\theta) + r + (x_o - r\theta) \tan\phi = 0 \qquad (3.3.1)$$

and

$$\hat{y}(\sin\theta + \tan\phi \cos\theta) + \hat{x}(\cos\theta - \tan\phi \sin\theta) + r\tan\phi = 0 \qquad (3.3.2)$$

Solving these for $\hat{x},\hat{y}$ we obtain the parametric representation of the envelope of L, relative to the wheel W. The envelope equation represented by these two

parametric equations is indeed the involute of a circle, since the locus of the center of the curvature of E is a circle having the equation

$$x_c^2 + y_c^2 = r^2 \sin^2\phi \qquad (3.3.3)$$

This circle is the base circle of the involute. The pressure angle ψ is the complement of the angle ϕ of the step's inclination.

4. ENVELOPE OF INVOLUTE PROFILE CUTTER

4.1 Introduction

As a final example of determining an analytical representation of the envelope of a family of curves, consider the case of spur gear tooth generation by shaping. This process can be modeled by two rolling disks, one having penetrating involute profile teeth and the other a gear blank to be cut. The task is to determine an expression that describes the "footprint" of the cutter onto the gear blank, and then to show that the footprint is of involute shape. Note that because of the constant profile shape along the width of the disks, the problem is reduced to two dimensions.

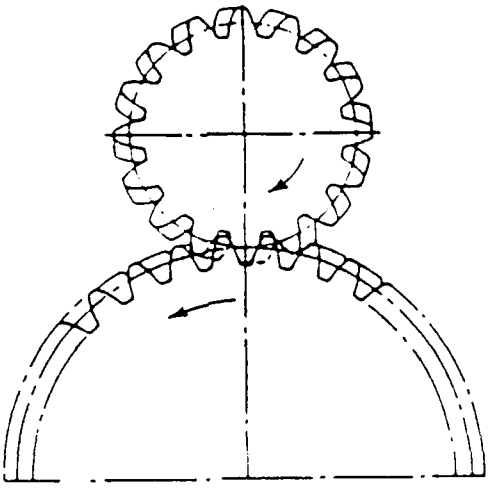

Figure 4.1 Spur Gear Shaping.

4.2 Involute Analysis

The parametric equations of an involute curve in rectangular coordinates may be described as follows:

Consider an arbitrary point P on the involute curve located by a position vector **p** as in Figure 4.2.1. Then **p** may be expressed as:

$$\mathbf{p} = r\mathbf{n}_r + r\phi\mathbf{n}_\theta \qquad (4.2.1)$$

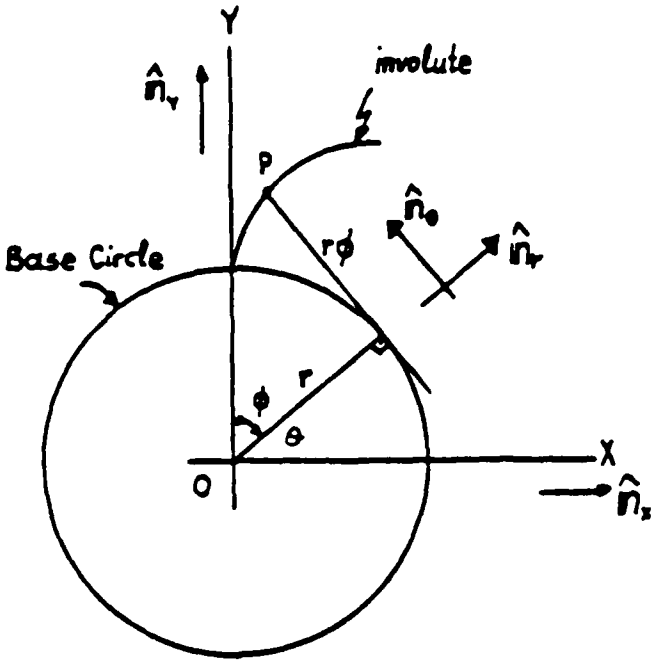

Figure 4.2.1 Involute Curve

where n_r and n_θ are unit vectors as shown, r is the generating base circle radius and ϕ is the involute angle. The coordinate axes are X and Y and n_x and n_y are unit vectors parallel to these axes. The unit vectors are then related to one another by the expressions:

$$n_r = \cos\theta n_x + \sin\theta n_y \qquad (4.2.2.a)$$

$$n_\theta = -\sin\theta n_x + \cos\theta n_y \qquad (4.2.2.b)$$

where θ is the inclination angle of n_r as shown.

Equation 4.2.1 may then be written as

$$p = (r\cos\theta - r\phi\sin\theta)n_x + (r\sin\theta + r\phi\cos\theta)n_y \qquad (4.2.3)$$

However

$$\theta + \phi = \frac{\pi}{2} \tag{4.2.4.a}$$

Hence,

$$\cos\theta = \cos(\frac{\pi}{2} - \phi) = \sin\phi \tag{4.2.4.b}$$

and

$$\sin\theta = \sin(\frac{\pi}{2} - \phi) = \cos\phi \tag{4.2.4.c}$$

Therefore from Equation (4.2.3) **p** becomes

$$\mathbf{p} = (r\sin\phi - r\phi\cos\phi)n_x + (r\cos\phi + r\phi\sin\phi)n_y \tag{4.2.5}$$

The parametric equations of the involute line in rectangular coordinates are then

$$x = r\sin\phi - r\phi\cos\phi \tag{4.2.6}$$

and

$$y = r\cos\phi + r\phi\sin\phi \tag{4.2.7}$$

or

$$y = f(x)$$

with slope

$$\frac{dy}{dx} = \frac{\frac{dy}{d\phi}}{\frac{dx}{d\phi}} = \cot\phi \tag{4.2.7.a}$$

4.3 Rolling Analysis

Consider two rolling wheels w_1 and w_2 of unequal radii as shown in Figure 4.3.1

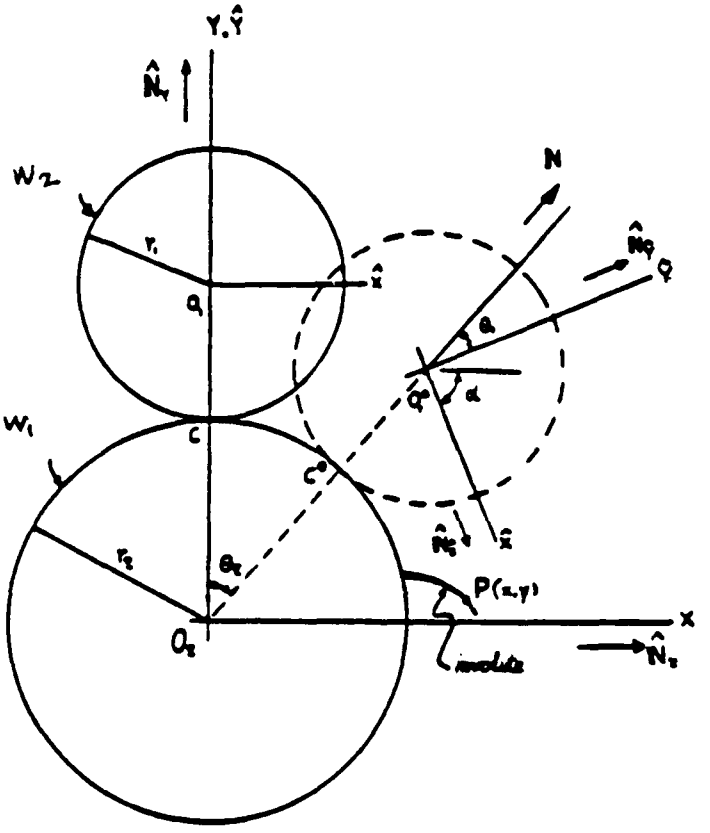

Figure 4.3.1 Rolling of Gear Blank over an Involute Profile Cutter

Let wheel w_1 be the cutter, and with a tooth of involute profile attached to it. Let wheel w_2 be the gear blank which rolls on the cutter and eventually over the involute curve. Consider a point P on the involute with coordinates x,y. The coordinate system $(\hat{X}\text{-}\hat{Y})$ is fixed on wheel w_2. Consider wheel w_2 at position O_1^* making an angle θ_2 with the Y axis. Angle θ_1 is measured between the $\hat{Y}$ axis and the line $O_2O_1^*$ making an angle θ_2 with the Y axis. Angle θ_1 is measured between

the $\hat{Y}$ axis and the line $O_2O_1^*$ of the centers. $\mathbf{N}_x, \mathbf{N}_y$ are unit vectors along the X-Y axes and $\mathbf{N}_{\hat{x}}, \mathbf{N}_{\hat{y}}$ are unit vectors along the $\hat{X}$-$\hat{Y}$ axes. The position vector $\mathbf{p}$ P is then

$$\mathbf{p} = x\mathbf{N}_x + y\mathbf{N}_y = \mathbf{O_2O_1^*} + \mathbf{p}^* \tag{4.3.1}$$

where $\mathbf{p}^*$ is the position vector of p relative to $\hat{X}, \hat{Y}$ at the O_1^* position.

Using the geometry from Figure 4.3.1 we can write:

$$\mathbf{p} = (r_1 + r_2)\mathbf{N} + \hat{x}\mathbf{N}_x + \hat{y}\mathbf{N}_y$$

where $\hat{N}$ is a unit vector along the line of centers of the wheels as shown. Expressing $\mathbf{p}$ in terms of the unit vectors $\mathbf{N}_x, \mathbf{N}_y$ in X-Y we have:

$$\mathbf{p} = [(r_1 + r_2)\sin\theta_2 + \hat{x}\cos\alpha]\mathbf{N}_{\hat{x}} + [(r_1 + r_2)\cos\theta_2 - \hat{x}\sin\alpha]\,\mathbf{N}_{\hat{y}} \tag{4.3.2}$$

Thus the coordinates of P with respect to the X-Y coordinate system may be written as:

$$x = (r_1 + r_2)\sin\theta_2 + \hat{x}\cos\alpha + \hat{y}\sin\alpha \tag{4.3.4.a}$$

$$y = (r_1 + r_2)\cos\theta_2 - \hat{x}\sin\alpha + \hat{y}\cos\alpha \tag{4.3.4.b}$$

solving for $\hat{x}, \hat{y}$ we have:

$$\hat{x} = x\cos\alpha - y\sin\alpha + (r_1 + r_2)\sin(\alpha - \theta_2) \tag{4.3.4.a}$$

$$\hat{y} = x\sin\alpha + y\cos\alpha - (r_1 + r_2)\cos(\alpha - \theta_2) \tag{4.3.4.b}$$

To simplify these equations, suppose $r_1 = r_2 = r$, then $\theta_2 = \frac{\alpha}{2}$ and

$$x = \hat{x}\cos\alpha + \sin\alpha + 2r\sin\frac{\alpha}{2} \qquad (4.3.6.a)$$

$$y = -\hat{x}\sin\alpha + \hat{y}\cos\alpha + 2r\cos\frac{\alpha}{2} \qquad (4.3.6.b)$$

and

$$\hat{x} = x\cos\alpha - y\sin\alpha + 2r\sin\frac{\alpha}{2} \qquad (4.3.7.a)$$

$$\hat{y} = x\sin\alpha + y\cos\alpha - 2r\cos\frac{\alpha}{2} \qquad (4.3.7.b)$$

4.4 Envelope Analysis

Suppose $y=f(x)$ describes a curve (that is, an involute tooth profile) in wheel w_1. Then this curve will have in the coordinate system of wheel w_2 a form expressed as

$$y(\hat{x},\hat{y},\alpha) = f[x(\hat{x},\hat{y},\alpha)] \qquad (4.4.1)$$

where $y(\hat{x},\hat{y},\alpha)$ and $x(\hat{x},\hat{y},\alpha)$ are given by equations (4.3.4) and (4.3.6). Equation (4.4.1) can be rewritten in the form

$$F(\hat{x},\hat{y},\alpha) = 0 \qquad (4.4.2)$$

Then the envelope of the curves in w_2 is given by the intersection of the surface of Equation (4.4.2) and the surface defined by the equation:

$$\frac{\partial F(\hat{x},\hat{y},\alpha)}{\partial\alpha} = 0 \qquad (4.4.3)$$

4.5 Envelope of Involute

Suppose the involute curve of Equations (4.2.6) and (4.2.7) is written as

$$y = f(x) \tag{4.5.1}$$

From Figure 4.3.1 it is observed that

$$\theta_1 = \left(\frac{r_2}{r_1}\right) \theta_2 \tag{4.5.2}$$

and

$$\alpha = \theta_1 + \theta_2 = \left(\frac{r_2}{r_1} + 1\right) \theta_2 = \frac{r_1 + r_2}{r_1} \theta_2 \tag{4.5.2.a}$$

Hence

$$\theta_2 = \frac{r_1}{r_1 + r_2} \theta_1 \tag{4.5.3}$$

Using Equations (4.3.4) and the above expression, Equation (4.5.1) takes the form:

$$(r_1 + r_2)\cos\left[\left(\frac{r_1}{r_1 + r_2}\right)\alpha\right] - \hat{x}\sin\alpha + \hat{y}\cos\alpha =$$

$$f\left\{(r_1 + r_2)\sin\left[\left(\frac{r_1}{r_1 + r_2}\right)\alpha\right] + \hat{x}\cos\alpha + \hat{y}\sin\alpha\right\} \tag{4.5.4}$$

Hence, by differentiating with respect to α, we have:

$$- r_1 \sin\left[\left(\frac{r_1}{r_1 + r_2}\right)\alpha\right] - \hat{x}\cos\alpha - \hat{y}\sin\alpha =$$

$$\frac{df}{dx}\left[r_1\cos\left[\left(\frac{r_1}{r_1 + r_2}\right)\alpha\right] - \hat{x}\sin\alpha + \hat{y}\sin\alpha\right] \qquad (4.5.5)$$

However, from Equations (4.3.4), (4.5.2), (4.5.3), and (4.2.7a) we have

$$\hat{x}\cos\alpha + \hat{y}\sin\alpha = x - (r_1 + r_2)\sin\left[\left(\frac{r_1}{r_1 + r_2}\right)\alpha\right] \qquad (4.5.6)$$

$$- \hat{x}\sin\alpha + \hat{y}\cos\alpha = y - (r_1 + r_2)\cos\left[\left(\frac{r_1}{r_1 + r_2}\right)\alpha\right] \qquad (4.5.7)$$

and

$$\frac{df}{dx} = \cot\phi$$

Hence, Equation (4.5.5) becomes:

$$- x\sin\phi + r_2\sin\left[\left(\frac{r_1}{r_1 + r_2}\right)\alpha\right]\sin\phi = y\cos\phi - r_2\cos\left[\left(\frac{r_1}{r_1 + r_2}\right)\alpha\right]\cos\phi$$

or

$$x\sin\phi + y\cos\phi = r_2\cos\left[\phi - \left(\frac{r_1}{r_1 + r_2}\right)\alpha\right] \qquad (4.5.8)$$

Observe though that from Equations (4.2.6) and (4.2.7) of the involute we have

$$x\sin\phi + y\cos\phi = r_2\sin^2\phi - r_2\phi\cos\phi\sin\phi + r_2\cos^2\phi + r_2\phi\sin\phi\cos\phi$$

or

$$x\sin\phi + y\cos\phi = r_2 \tag{4.5.9}$$

Comparing Equations (4.5.8) and (4.5.9) we note that in order for the right sides to be equal, we must have:

$$\cos\left[\phi - \left(\frac{r_1}{r_1 + r_2}\right)\alpha\right] = 1$$

or

$$\phi = \left(\frac{r_1}{r_1 + r_2}\right)\alpha \tag{4.5.10}$$

Next, examine the involute curve in w_2 in terms of $\hat{x}$ and $\hat{y}$:
From Figure 6.3.1 we note that

$$\alpha - \theta_2 = \left(\frac{r_1}{r_1 + r_2}\right)\alpha \tag{4.5.11}$$

From Equations (4.3.5) we have:

$$\hat{x} = x\cos\alpha - y\sin\alpha + (r_1 + r_2)\sin\left[\left(\frac{r_1}{r_1 + r_2}\right)\alpha\right] \tag{4.5.12.a}$$

and

$$\hat{y} = x\sin\alpha + y\cos\alpha - (r_1 + r_2)\cos\left[\left(\frac{r_1}{r_1 + r_2}\right)\alpha\right] \qquad (4.5.12.b)$$

Then from Equations (4.2.6) and (4.2.7) we can substitute x and y for functions of ϕ. This leads to:

$$\hat{x} = r_2\sin\phi\cos\alpha - r_2\phi\cos\phi\cos\alpha - r_2\cos\phi\sin\alpha - r_2\phi\sin\phi\sin\alpha + (r_1+r_2)\sin\left(\frac{r_1}{r_1 + r_2}\right)\alpha$$

and

$$\hat{y} = r_2\sin\phi\sin\alpha - r_2\phi\cos\phi\sin\alpha + r_2\cos\phi\cos\alpha + r_2\sin\phi\cos\alpha - (r_1+r_2)\cos\left(\frac{r_1}{r_1 + r_2}\right)\alpha$$

or

$$\hat{x} = r_2\sin(\phi - \alpha) - r_2\phi\cos(\phi - \alpha) + (r_1 + r_2)\sin\left[\left(\frac{r_1}{r_1 + r_2}\right)\alpha\right] \qquad (4.5.13.a)$$

and

$$\hat{y} = r_2\cos(\phi - \alpha) + r_2\phi\sin(\phi - \alpha) - (r_1 + r_2)\cos\left[\left(\frac{r_1}{r_1 + r_2}\right)\alpha\right] \qquad (4.5.13.b)$$

Observe from Equation (4.5.10) that

$$\phi - \alpha = \left(\frac{r_1}{r_1 + r_2}\right)\alpha - \alpha = -\left(\frac{r_2}{r_1 + r_2}\right)\alpha$$

and

$$\phi - \alpha = -\left(\frac{r_2}{r_1}\right)\phi \qquad (4.5.14)$$

Hence, Equations (4.5.13) become:

$$\hat{x} = r_1 \sin\left(\frac{r_2}{r_1}\phi\right) - r_2\phi\cos\left(\frac{r_2}{r_1}\phi\right)$$

and

$$\hat{y} = -r_1\cos\left(\frac{r_2}{r_1}\phi\right) - r_2\phi\sin\left(\frac{r_2}{r_1}\phi\right)$$

Using the substitution

$$\left(\frac{r_2}{r_1}\right)\phi = \beta \qquad (4.5.15)$$

we obtain:

$$\hat{x} = r_1\sin\beta - r_1\beta\cos\beta \qquad (4.5.16.a)$$

and

$$\hat{y} = -r_1\cos\beta - r_1\beta\sin\beta \qquad (4.5.16.b)$$

Observe by comparison with Equations (4.2.6) and (4.2.7), that Equations (6.5.16) describe an involute on wheel w_2 going downwards. Thus the footprint of the involute profile of the cutter tooth on the gear blank is seen to be of involute shape.

5. COMPUTER SIMULATION OF MANUFACTURING PROCESSES

5.1 Introduction

Although the analytical development of the involute profile of a spur gear tooth is relatively simple, the analogous development for bevel gears is much more cumbersome. An alternative to the analytical development is to use computer graphics technology. A feature of this technology is "solid modeling" which is used for developing geometry for finite element analyses. The settings and parameters of the gear manufacturing processes may be specified to simulate the motion of a cutter and gear blank. Thus analytical expressions of the geometry are not needed.

For an accurate analysis, the computer model cut gear tooth must be an accurate model of the actual manufactured gear tooth. To obtain such a model it is necessary to have exact specifications and dimensions of the cutting tool and gear blank, the relative positions of the two gears and their motion relative to each other.

This part of the report discusses computer simulation of gear manufacturing procedures. It is shown that this method accurately defines the geometry of the gear tooth surfaces. The method will be demonstrated through a series of examples.

The software used is the solid modeling family in the SDRC I-DEAS package, called GEOMOD [13]. GEOMOD provides the user with a set of modular software

tools to aid in the generation of geometric design of a mechanical system. In particular, object modeling is a module where the user can create 3-dimensional geometric shapes and manipulate the geometry by deforming, orienting, joining, and cutting objects with one another. Overall, the package offers a powerful tool, for defining and evaluating the geometry of a structural component or system.

5.2 Gear and Straight Sided Rack

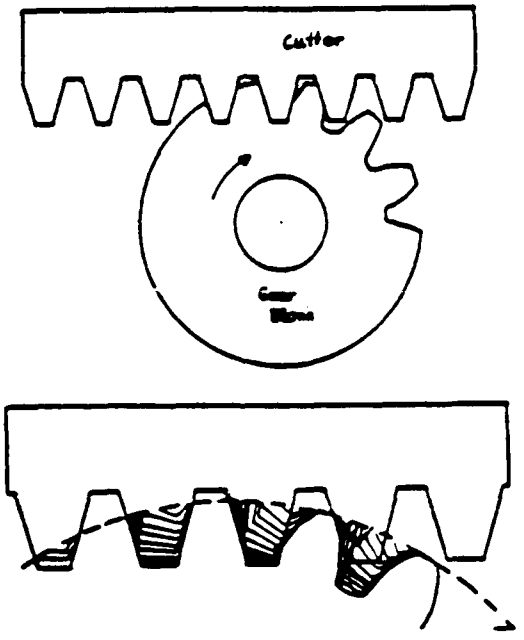

Figure 5.2.1 Rack and Spur Gear - Generating Process

The generating process of forming involute gear teeth is shown in Figure 5.2.1, where a gear blank and a rack cutter are shown. The cutting process occurs as the cutter moves horizontally and the gear blank rolls upon it. Gear

The teeth formed are the "footprint" of the rack onto the gear blank [18]. Figure 5.2.2 illustrates the concept of the "footprint".

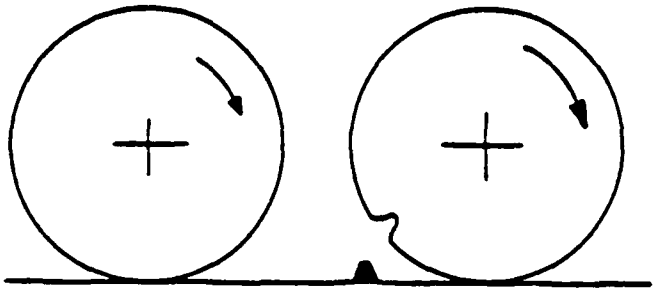

Figure 5.2.2 Footprint of a Step on the Wheel Rolling Over It

Applying this procedure with solid modeling we create two objects: the gear blank (a cylinder of radius equal to the outside radius of the gear) and the cutter. Figure 5.2.3 shows the straight sided rack cutter. Figure 5.2.4 shows the position of the cutter before and after the rolling motion. It also shows the gear blank with the "footprint". Figure 5.2.5 shows two spur gear teeth generated by the process.

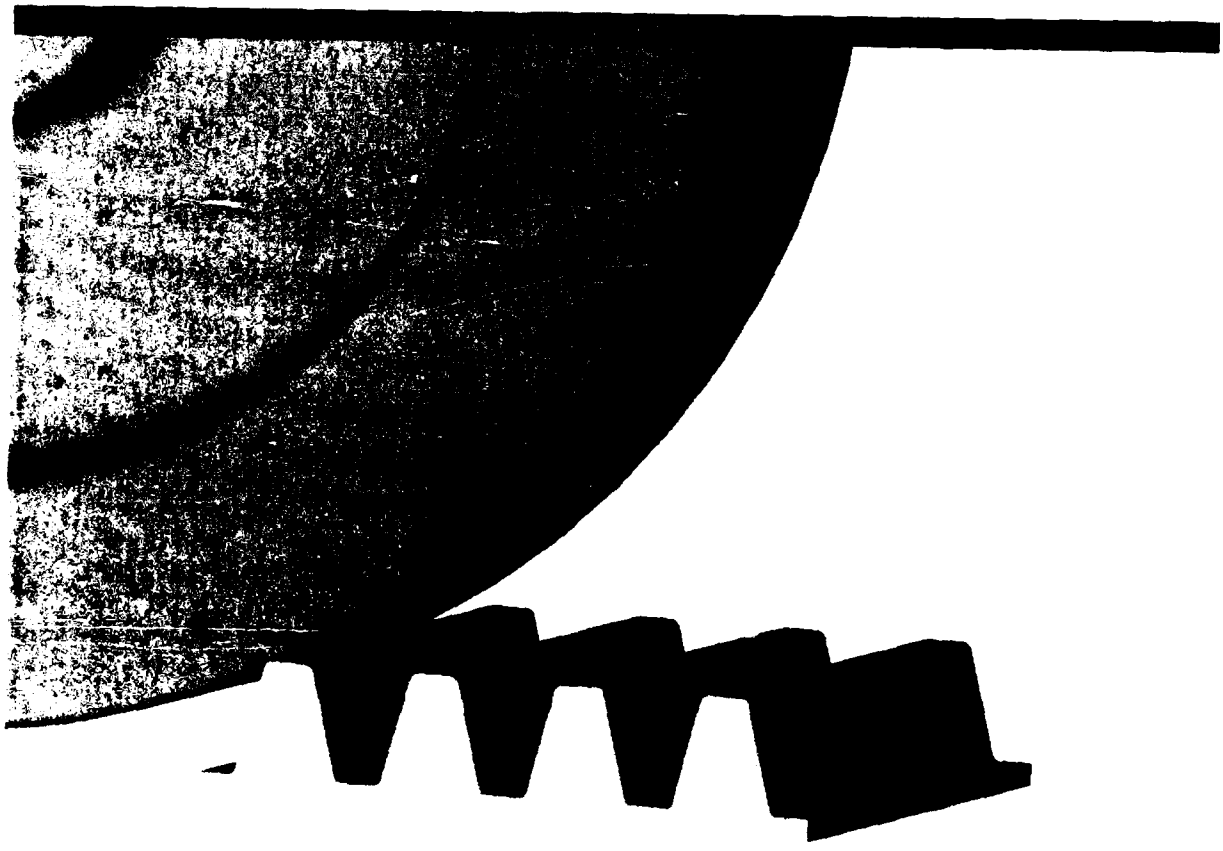

Figure 5.2.3 Solid Model of Straight Sided Rack Cutter

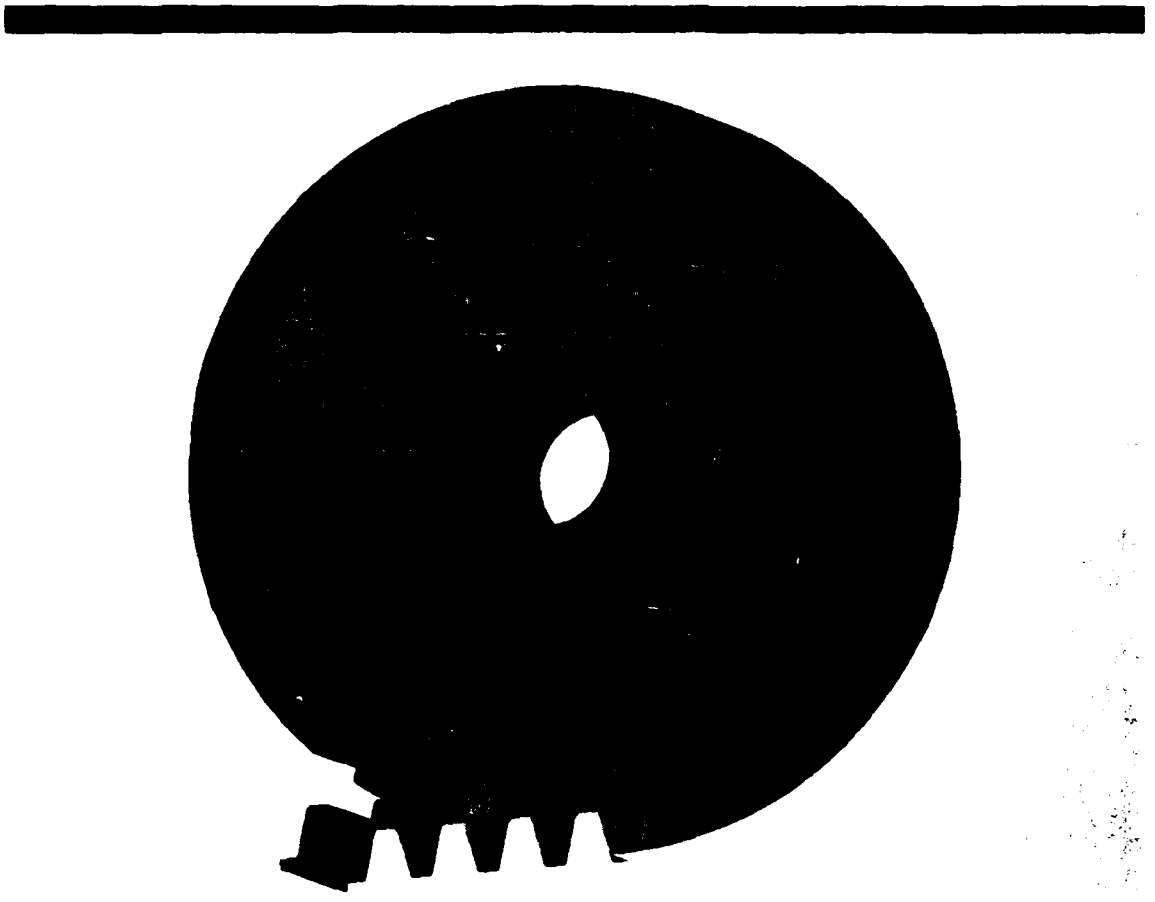

Figure 5.2.4 Solid Model of Gear Blank and Rack Cutter

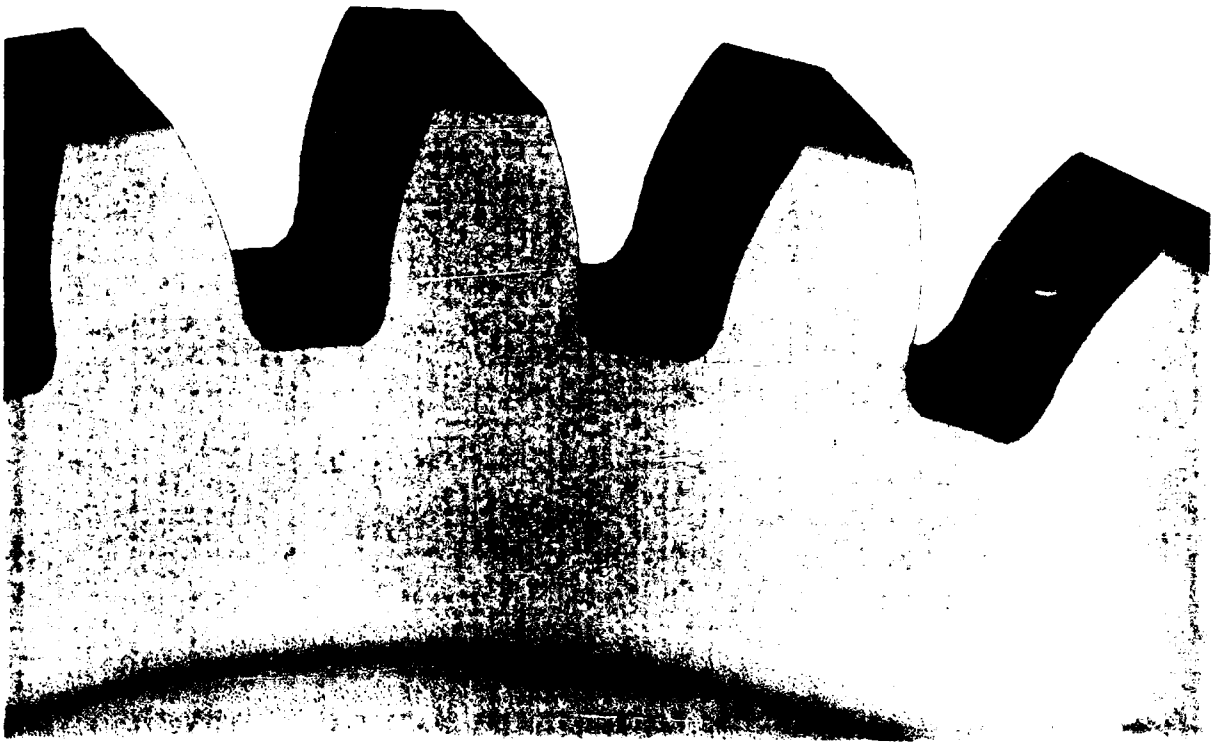

Figure 5.2.5 Solid Model of Resulting Spur Gear Tooth

What remains to be shown is that the profile of the generated tooth surface is of true involute shape. To see this the coordinates of points on the generated curve profile must be calculated and compared with those of an involute curve.

At each time step of the cutting process, a facet on the tooth surface is created. The coordinates of points on the facets may be extracted during the generation process. At the same time, the angle between a line from the origin to the point of intersection between the tangent to the base circle and the Y

involute curve to obtain an analytical description of the matching involute that is:

$$x = r \sin\phi - r\,\phi \cos\phi \qquad (5.2.1)$$

and

$$y = r \cos\phi + r\,\phi \sin\phi \qquad (5.2.2)$$

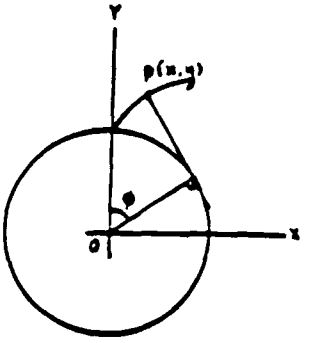

Figure 5.2.6 Coordinates of Points of an Involute Curve

Figure 5.2.7 shows a comparison of the two curves. It is seen that the two curves are the same. (In the figure the curves are offset for the purpose of comparison.)

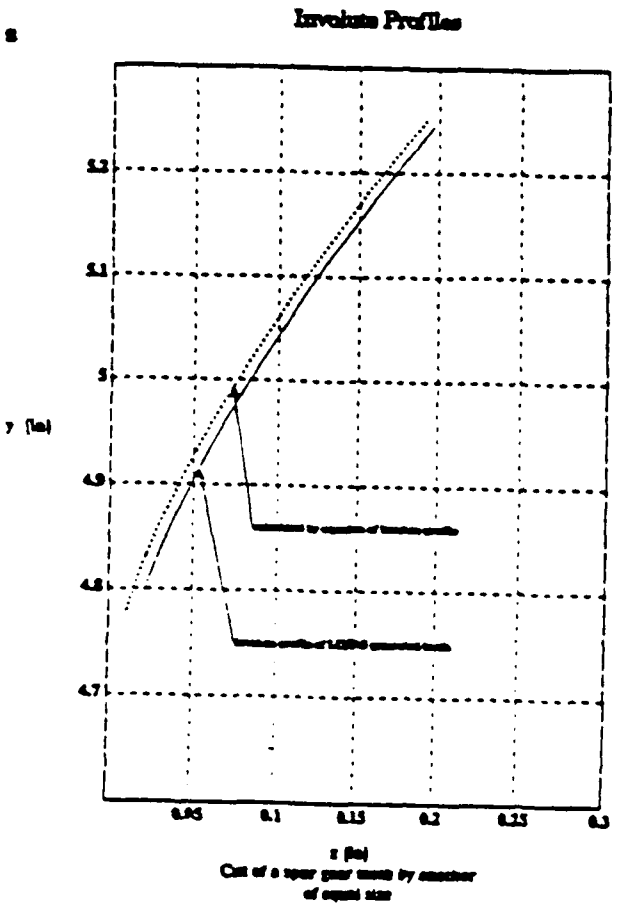

Figure 5.2.7 Generated and Calculated Involute Profiles

5.3 Involute Profile Cutter on a Wheel

The foregoing process may be generalized with the cutter tooth being an involute on a circular disk, as in Figure 5.3.1. Figures 5.3.2 to 5.3.5 show the resulting computer graphic simulation.

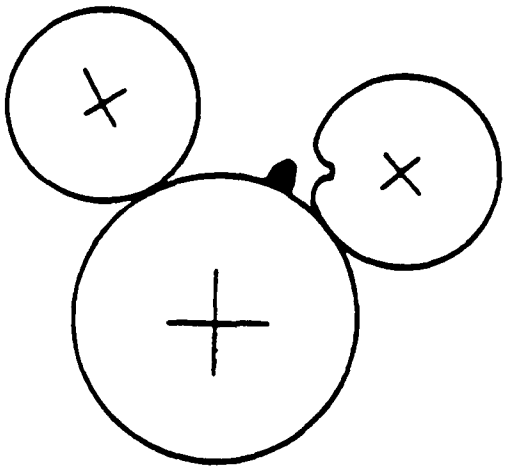

Figure 5.3.1 Footprint of an Involute Cutter on a Gear Blank

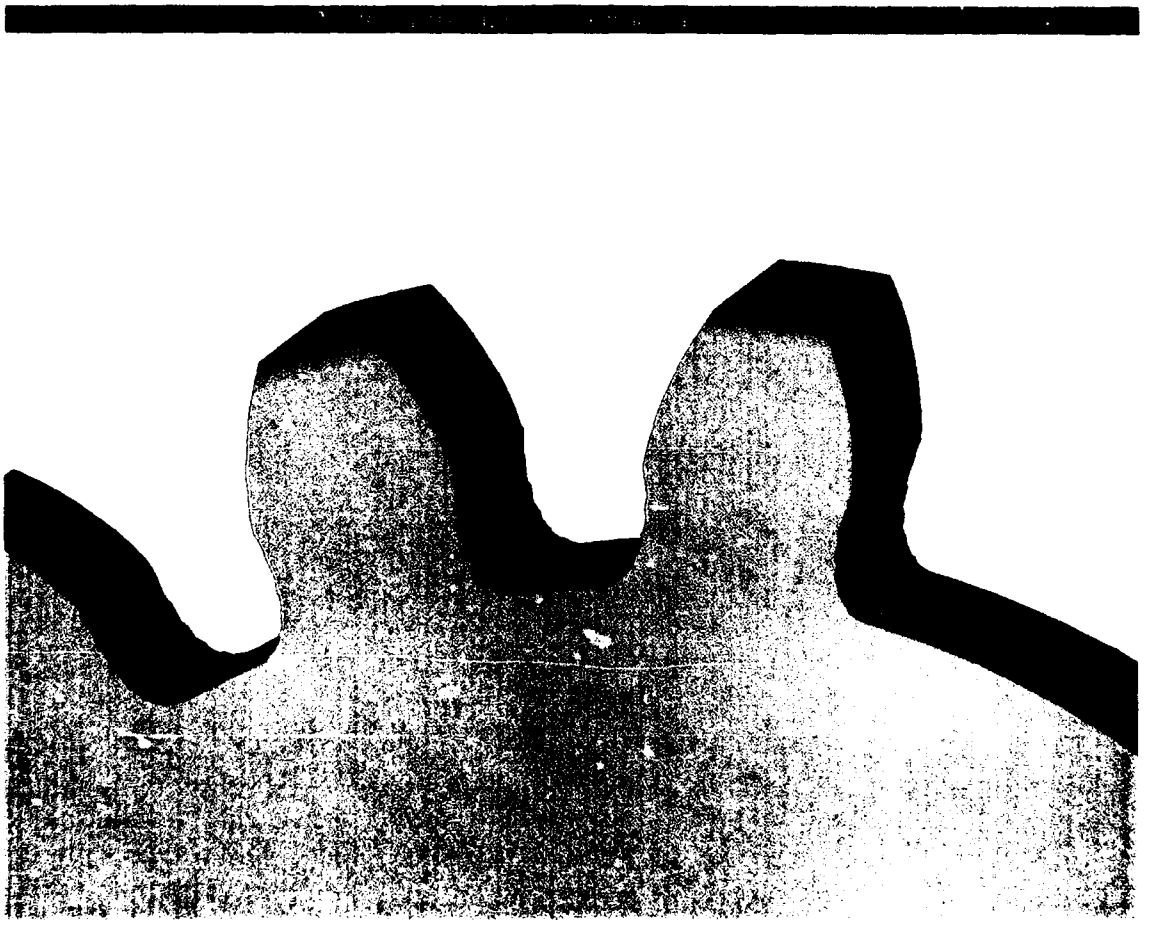

Figure 5.3.2 Solid Model of Cutter of [illegible]

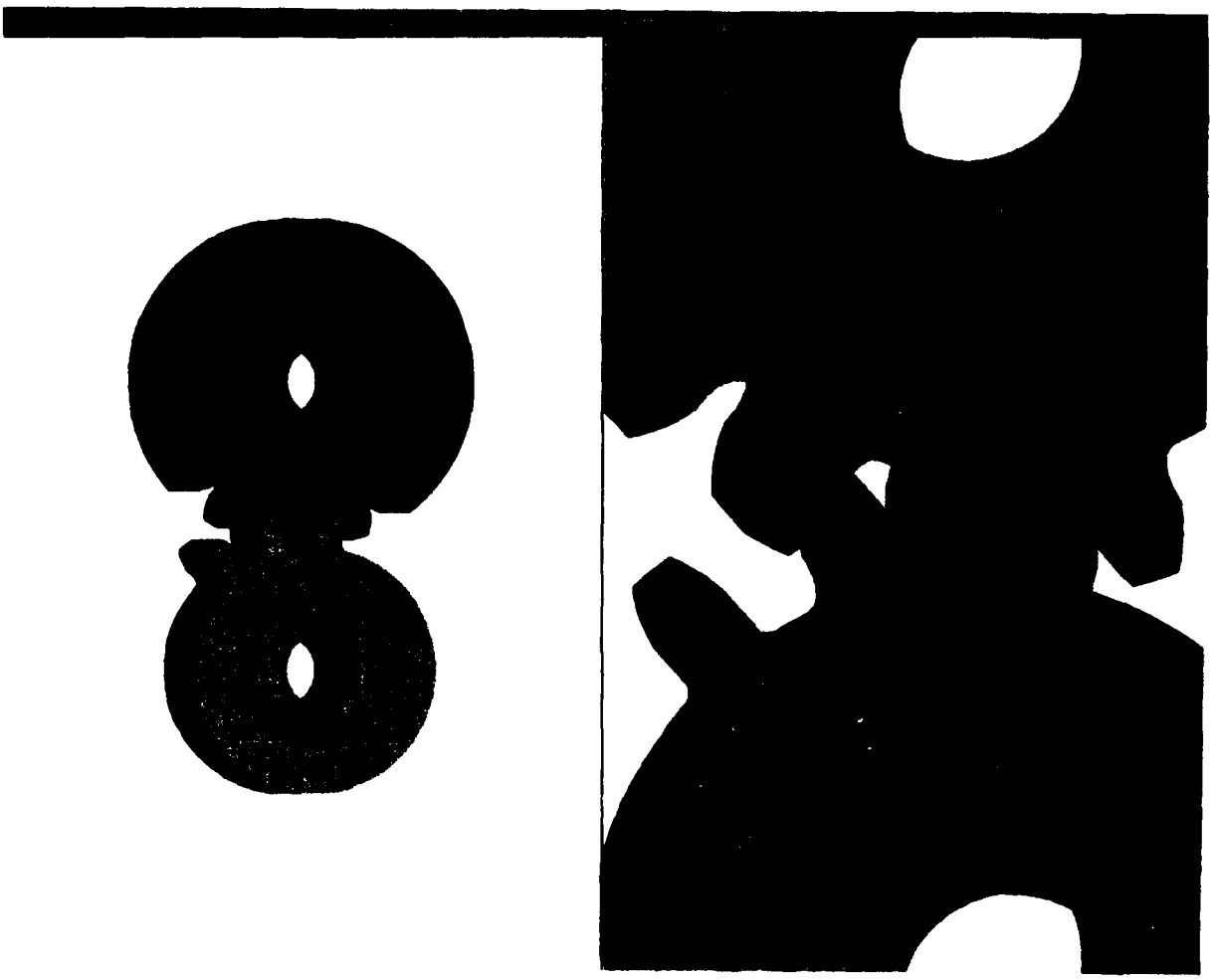

Figure 5.3.3 Generated Gears (Equal Radii)

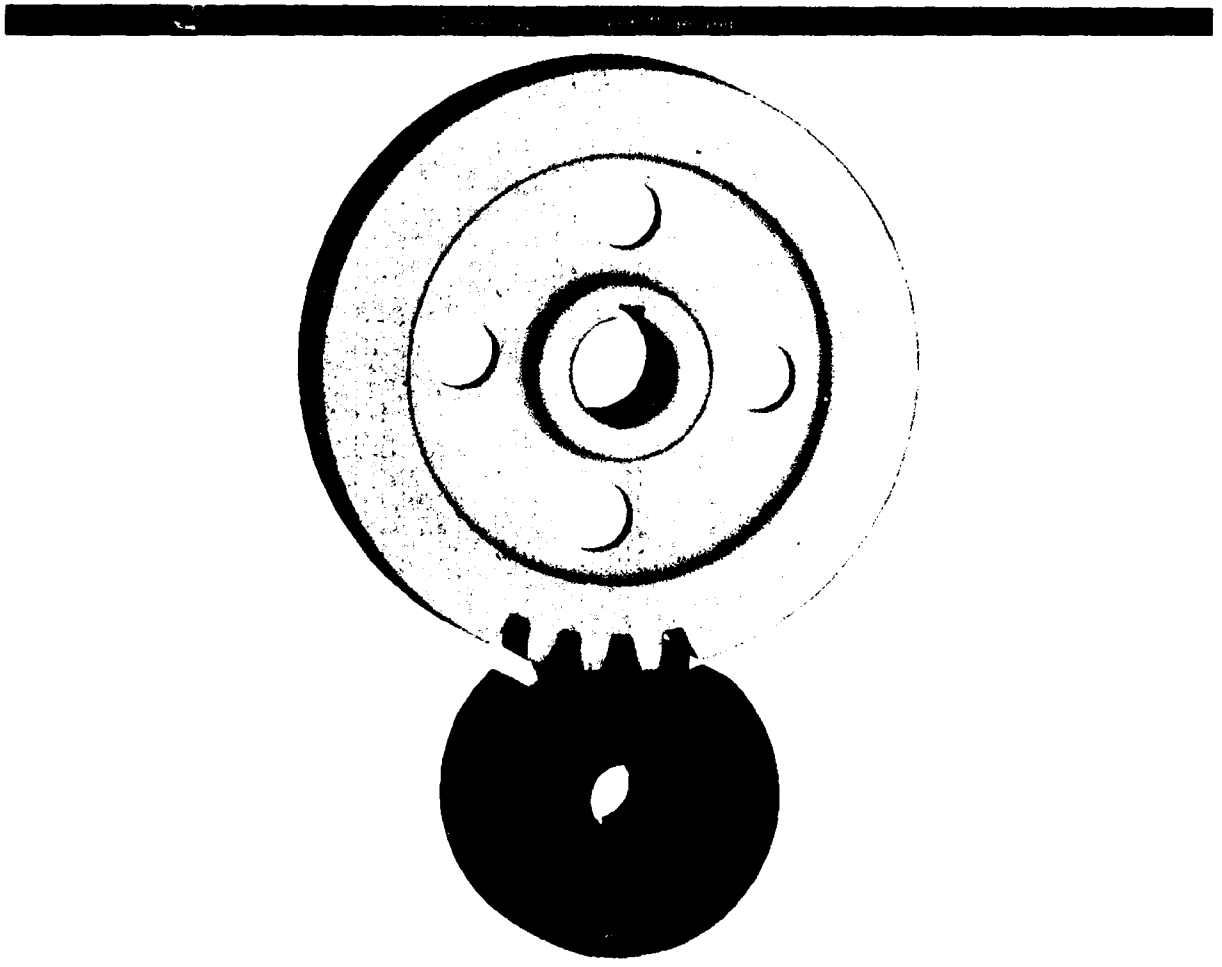

Figure 5.3.4 Generated Gears (Unequal Radii)

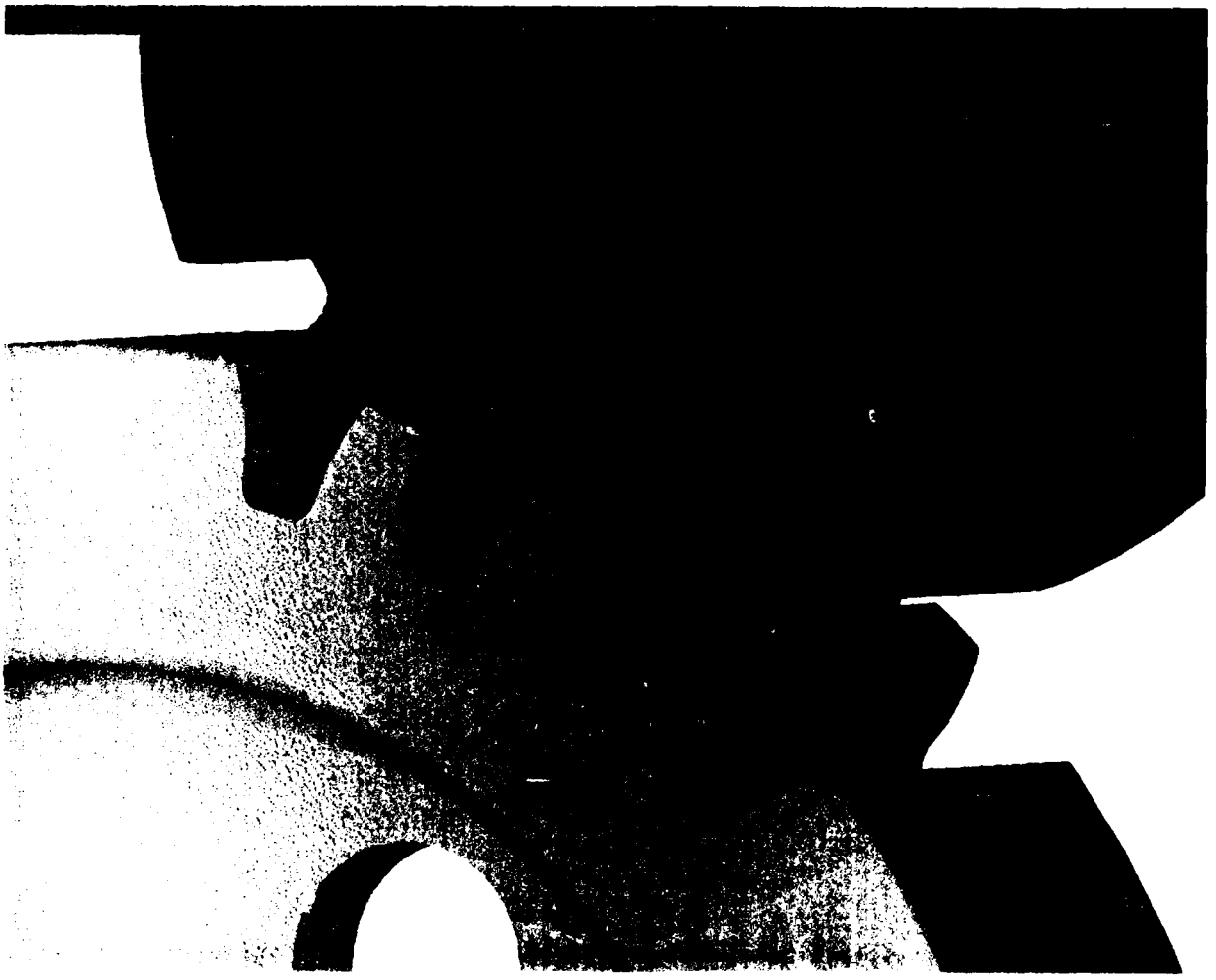

Figure 5.3.5 Close-up View of Generated Teeth

5.4 Straight Bevel Gears

Consider the extension of these concepts to the development of straight bevel gears. The involute profile of a spur gear tooth is generated from a "base circle". Extended in the axial direction, the set of base circles form a cylinder -- the "base cylinder". In an analogous manner, the basic rack for a spur gear becomes a "crown gear rack" for a bevel gear. For a bevel gear the base surface is a cone. See Figure 5.4.1.

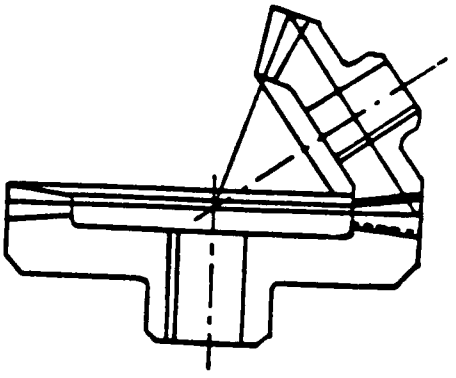

Figure 5.4.1 Bevel and Crown Gears

The pitch surface of the crown gear is planar. The teeth of the crown gear are straight sided with an inclination corresponding to the pressure angle. When generating methods are employed in manufacturing bevel gears, the relative motion specified for the cutting tool and the gear blank is the same as would be obtained if the bevel gear to be cut is rotating in mesh with the crown gear. This concept provides the procedure for computer solid modeling simulation of the straight bevel gear tooth.

The steps in this simulation are the same as those of the spur gear. Figure 5.4.2 shows a bevel gear blank and a crown gear cutter. Figures 5.4.3 to 5.4.5 show a generated tooth on a pinion.

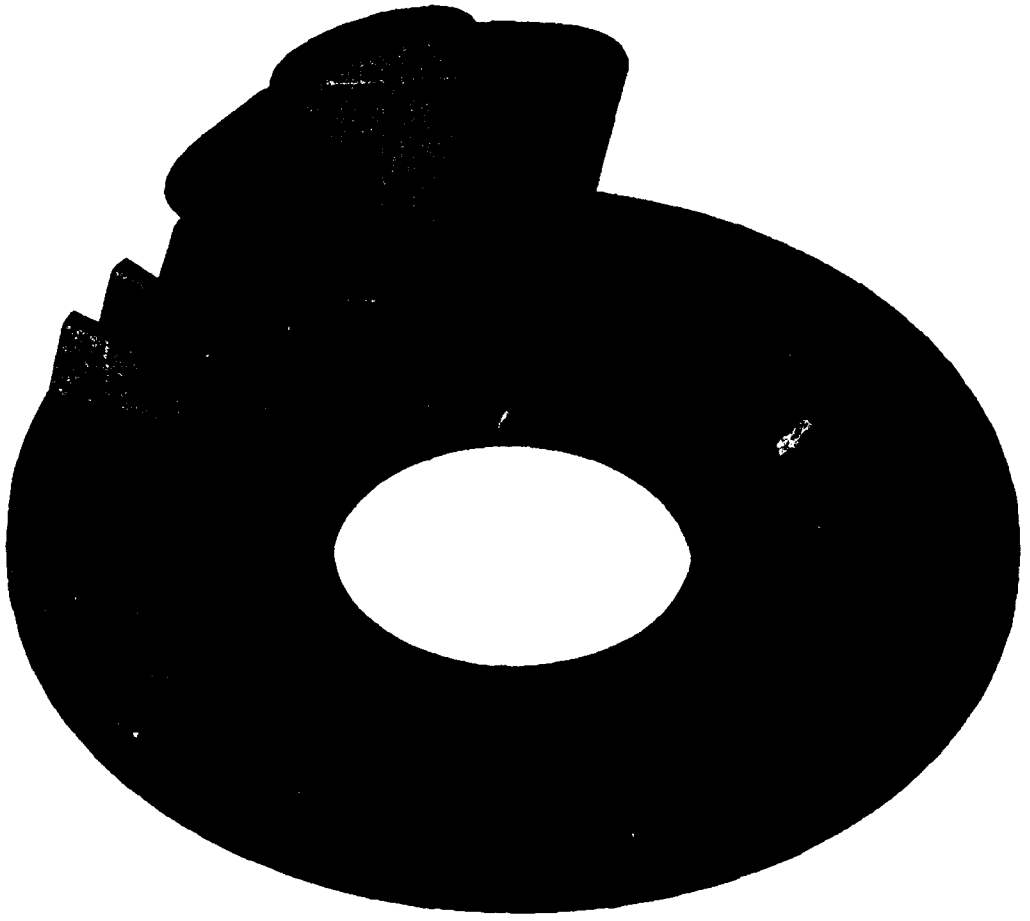

Figure 5.4.2 Solid Model of Pinion Blank and Crown Gear Cutter

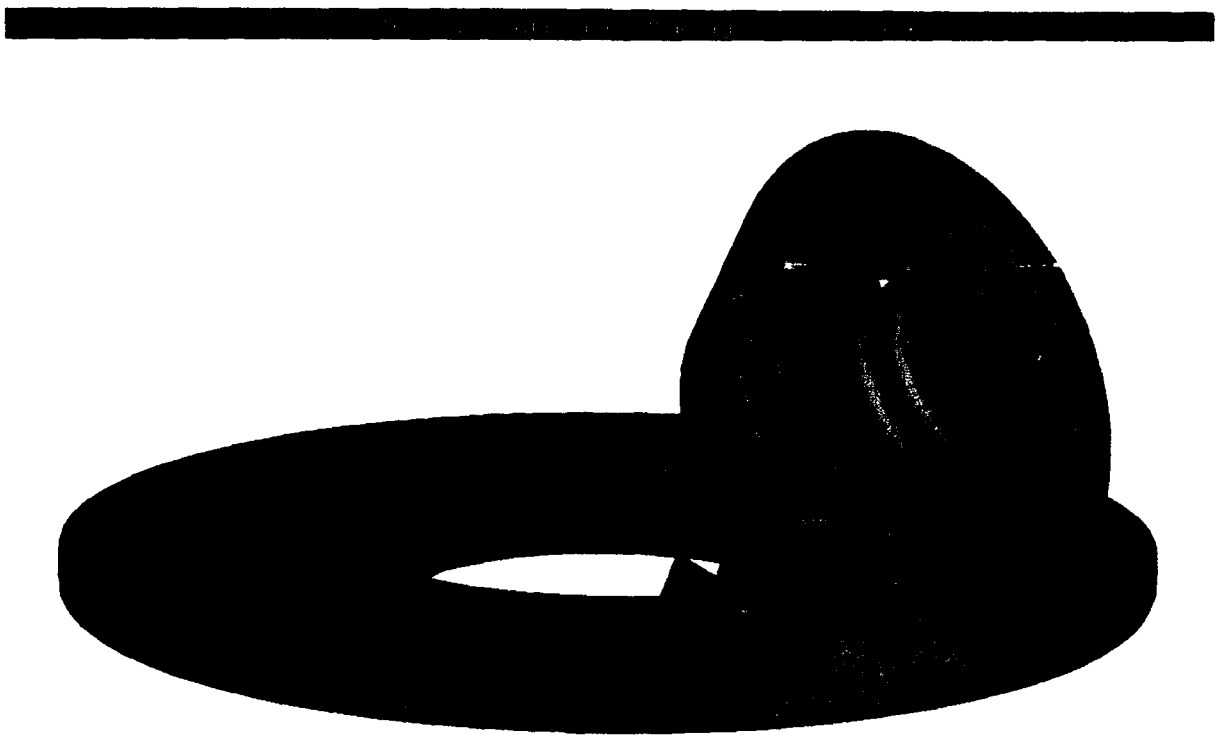

Figure 5.4.3 Cutter Before and After Cut and Pinion with Generated Tooth

Figure 5.4.4 Close-up View of the Cut Tooth on the Pinion Blank

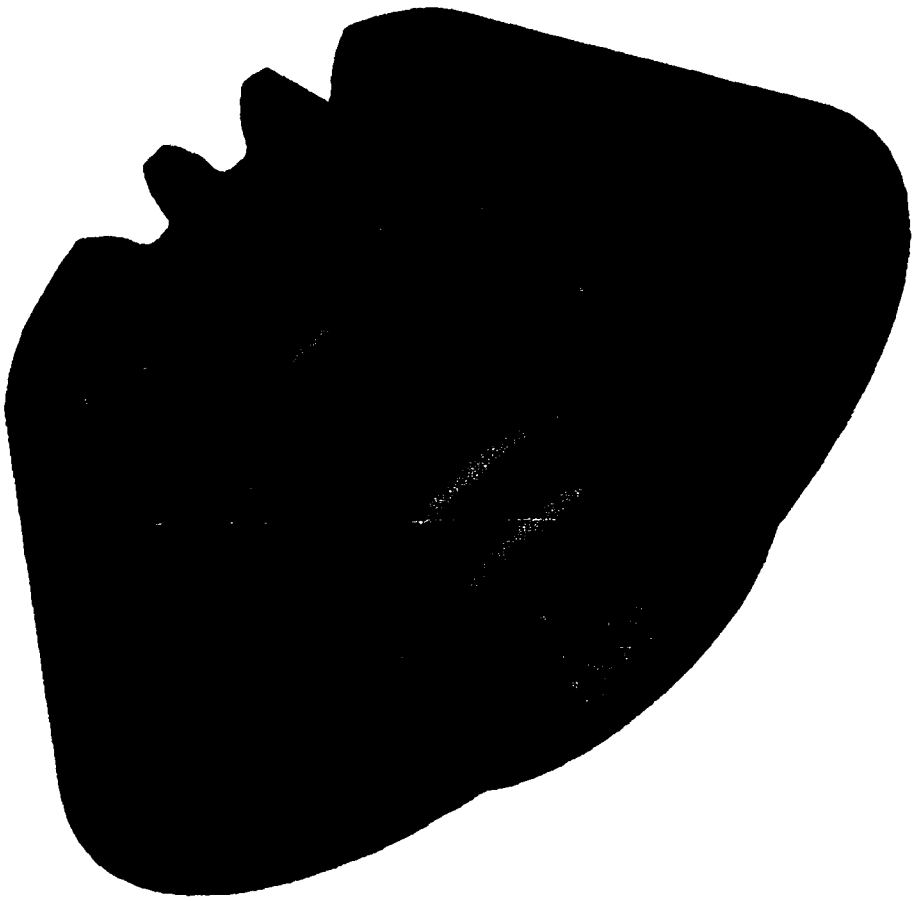

Figure 5.4.5 Pinion with Generated Teeth

DISCUSSION

The foregoing concepts establish the principles of a computer simulation of gear tooth manufacturing procedures. The analysis shows that gear tooth surfaces may be viewed as envelopes of gear cutters sweeping through the gear blank. The examples demonstrate the feasibility of computer based analysis and design of the cutting process.

The analysis is developed for spur gears. As such, it is a planar analysis. Even with the simplification of planar modeling, however, it is seen that the analysis is cumbersome. Indeed, a strictly analytical development of bevel gear surfaces -- particularly spiral bevel gear surfaces -- is virtually intractable. The computer simulation, however, is not restricted to a planar analysis. With the computer simulation, three-dimensional surfaces, such as occur with spiral bevel gear teeth, are developed in the same manner as two-dimensional spur gear tooth surfaces.

The value of the analysis is that it establishes the validity of the computer simulation. Hence, the surfaces of standard tooth forms can be developed. These surfaces in turn, can be used to develop finite element modeling of the gear teeth.

The capabilities of the computer analysis extend beyond this to the analysis of non-standard tooth forms and their associated fabrication procedures. That is, the procedure can be used to obtain a representative of non-standard

tooth surfaces. The fabrication procedure to develop these surfaces is a by-product of the simulation.

Finally, by extending the computer graphic analysis it is seen that it can be applied with other machine surfaces, such as cams and bearings.

CONCLUSIONS

1. The analysis demonstrates the utility of computer graphics in simulating gear design and manufacture. The use of these procedures eliminates the need to rely upon unwieldy analytical representations of gear tooth geometry. (Analytical representations have heretofore been intractable except for the simplest of gear tooth surfaces.)

2. The computer graphics representation is ideally suited for developing finite element models of gear teeth. (In the past, geometrical complexity has precluded an easy development of such models.)

3. The developed procedure may be used for conceptual exploration of new designs (that is, the cutter shape and movement) is an immediate byproduct of the graphics process.

REFERENCES

1. D. Mavriplis, "Computer Simulation and Analysis of Gear Teeth Manufacturing Processes," Ph.D. Dissertation, University of Cincinnati, Cincinnati, Ohio 45221, 1988.

2. S. H. Chang, R. L. Huston, and J. J. Coy, "Computer Aided Design of Bevel Gear Tooth Surfaces," NASA Technical Memorandum 101449 and AVSCOM Technical Memorandum 88-C-005, December, 1989.

3. S. H. Chang and R. L. Huston, "A Computer Aided Design Procedure for Generating Gear Teeth," Fourth International Power Transmission and Gearing Conference, ASME Paper No. 84-DET-184, Boston, MA, 1984.

4. W. C. Graustein, Differential Geometry, MacMillan, New York, 1935.

5. F. Litvin, W. Tsung, H. Lee, Generation of Spiral Bevel Gears with Conjugate Tooth Surfaces and Tooth Contact Analysis, NASA Technical Report 87-C-22, August 1987.

6. R. Drago, B. Uppaluri, G. Fries, Large Rotorcraft Transmission Technology Development Program, Volume I, Technical Report to NASA, 1982.

7. J. J. Coy, D. P. Townsend, and E. V. Zavetsky, Gearing, NASA Reference Publication 1152, AVSCOM Technical Report 84-C-15, December 1985.

8. American Gear Manufacturers Association, AGMA Design Manual for Bevel Gears, AGMA 330.01, Washington DC, 1972.

9. Y. Terauchi, K. Nagamura, W.-S. Peng, and H. Sentoku, Study of Bevel Gears - 1st Report, Theoretical Calculation of Tooth Bearing and Experiment, Bulletin of the JSME, Vol. 29, No. 250, 1986, pp. 1294-1302.

10. Y. Terauchi, K. Nagamura, W.-S. Peng, and H. Sentoku, Study of Tooth Bearing of Bevel Gears - 2nd Report, Relation Between Tooth Bearing and Assembly Error, Shaft Angle Error, Bulletin of the JSME, Vol. 29, No. 250, 1986, pp. 1303-1312.

11. J. E. Shigley and L. D. Mitchell, Mechanical Engineering Design, McGraw Hill, 1983, pp. 665-667.

12. R. H. MacNeal (Ed.), MSC/NASTRAN - Handbook for Linear Static Analysis, The MacNeal-Schwendler Corp., Los Angeles, 1985.

13. L. Peterson, Ed., MSC/NASTRAN - MSGMESH Analyst's Guide, The MacNeal-Schwendler Corp., Los Angeles, 1983.

14. Darle W. Dadley, Gear Handbook, McGraw Hill, 1962, First Edition, pp. 5.54-5.59, Table 5.22.

15. Gleason, Straight Bevel Gear Design, Gleason Works, Publication SD3160, 1972.

16. SDRC I-DEAS Geomod * Solid Modeling and Design, User's Guide (level 3), SDRC, Milford, Ohio.

17. S. H. Chang, R. L. Huston, and J. J. Coy, A Finite Element Stress Analysis of Spur Gears Including Fillet Radii and Rim Thickness Effects, Journal of Mechanics, Transmissions, and Automation in Design, Vol. 105, pp. 327-330, September 1983.

18. SDRC I-DEAS, Supertab, Model Solutions, User's Guide, level 3, Structural Dynamics Research Corp., Milford, 1987.

19. R. L. Huston and C. E. Passerello, Finite Element Methods: An Introduction, Marcel Dekker, 1984.

20. C. A. Brebbia, J.C. Telles, L. C. Wrobel, Boundary Element Techniques, Springer-Verlag, Berlin, 1984.

21. S. Oda, K. Nagamura, K. Aoki, Stress Analysis of Thin Rim Spur Gears by Finite Element Method, Bulletin of JSME, Vol. 24, No. 193, July 1981, pp. 1273-1280.

22. William C. Graustein, Differential Geometry, The MacMillan Company, New York, 1935.

23. S. Chang, R. L. Huston, and J. J. Coy, A Computer Aided Design Procedure for Generating Gear Teeth, ASME 24-DET-184, 1985.

24. Werner F. Vogel, Involutometry and Trigonometry, Michigan Tool Company, Detroit, 1945.

25. T. W. Khiralla, On the Involute Geometry of External Involute Spur Gears, C/I Leaming, California, 1976.

26. R. L. Huston and J. J. Coy, Ideal Spiral Bevel Gear - A New Approach to Surface Geometry, NASA Technical Memorandum 81446, 1980.

27. F. Litvin, K. Krylov, and M. Erichov, Generation of Tooth Surfaces by Two Parameter Enveloping, Mechanism and Design, Vol. 10, 1975, Pergamon Press, pp. 365-373.

28. R. L. Huston, Y. Lin, and J. J. Coy, Tooth Profile Analysis of Circular Cut, Spiral Bevel Gears, ASME 82-DET-79.

29. T. R. Kane, Analytical Elements of Mechanics, Academic Press, NY, 1961.

30. P. Altidis, M. Savage, Flexibility Effects on Tooth Contact Location in Spiral Bevel Gear Transmissions, NASA 4055, 1987.

31. W. Coleman, Design and Manufacturing of Spiral Bevel and Hypoid Gears for Heavy-Duty Drive Axles, SAE, January 1962.

32. A Dyson, A General Theory of the Kinematics and Geometry of Gears in Three Dimensions, Clapendon Press, Oxford, 1969.

33. W. Bultmann, Die Arbeitszeitermittlung der Vezzahnungsarbeiten, Springer-Verlag, Berlin, 1960.

34. Earle Buckingham, Analytical Mechanics of Gears, Dover Publications Inc., NY, 1949.

35. Formulas in Gearing, Brown & Sharpe Mfg. Co., 1936.

36. Luther P. Eisenhart, A Treatise on the Differential Geometry of Curves and Surfaces, Ginn and Company, 1909.

37. C. E. Weatherburn, Differential Geometry of Three Dimensions, University Press, London, 1927.

38. R. H. Fowler, The Elementary Differential Geometry of Curves, University Press, Cambridge, 1920.

39. Irving J. Levinson, Machine Design, Reston Publishing Company Inc., Virginia, 1978.

40. Dirk J. Struik, Classical Differential Geometry, Addison-Wesley Press, Cambridge, 1950.

41. Chuan-Chih Hsiung, A First Coarse in Differential Geometry, John Wiley & Sons, NY, 1981.

NASA
National Aeronautics and Space Administration

Report Documentation Page

1. Report No.	2. Government Accession No.	3. Recipient's Catalog No.
NASA CR-185200 AVSCOM TM 90-C-003		

4. Title and Subtitle	5. Report Date
Computer Simulation of Gear Tooth Manufacturing Processes	February 1990
	6. Performing Organization Code

7. Author(s)	8. Performing Organization Report No.
Dimitri Mavriplis and Ronald L. Huston	None
	10. Work Unit No. 1L162209A47A 505-63-51

9. Performing Organization Name and Address	11. Contract or Grant No.
University of Cincinnati Department of Mechanical and Industrial Engineering Cincinnati, Ohio 45221-0072	NSG-3188

12. Sponsoring Agency Name and Address	13. Type of Report and Period Covered
Propulsion Directorate U.S. Army Aviation Research and Technology Activity—AVSCOM Cleveland, Ohio 44135-3127 and NASA Lewis Research Center Cleveland, Ohio 44135-3191	Contractor Report Final
	14. Sponsoring Agency Code

15. Supplementary Notes

Project Manager, Fred B. Oswald, Propulsion Systems Division, NASA Lewis Research Center.

16. Abstract

This report discusses the use of computer graphics to simulate gear tooth manufacturing procedures. An analytical basis for the simulation is established for spur gears. The simulation itself, however, is developed not only for spur gears, but for straight bevel gears as well. The applications of the developed procedure extend from the development of finite element models of heretofore intractable geometrical forms, to exploring the fabrication of nonstandard tooth forms.

17. Key Words (Suggested by Author(s))	18. Distribution Statement
Computer-aided design; Computer graphics; Spur gears; Bevel gears; Gear tooth profile	Unclassified – Unlimited Subject Category 37

19. Security Classif. (of this report)	20. Security Classif. (of this page)	21. No. of pages	22. Price*
Unclassified	Unclassified	52	A04

NASA FORM 1626 OCT 86

*For sale by the National Technical Information Service, Springfield, Virginia 22161